Caustics from Optical Conformal Mappings

Huiyan Peng and Huanyang Chen[*]

Institute of Electromagnetics and Acoustics and Key Laboratory of Electromagnetic Wave Science and Detection Technology, Xiamen University, Xiamen, 361005, China

In this article, we propose transformation caustics by applying coordinate transformation to the caustic effect. The limit boundaries of caustics can be used to design devices with asymmetric light propagation or light confinement, thus providing an alternative degree of freedom for metamaterials.

I. INTRODUCTION

The caustic effect is an envelope boundary effect of light rays that are reflected or refracted by curved surfaces, interfaces, or objects. It has been extensively studied in geometric optics, differential geometry, and even computer science and the arts [1]. Such an envelope effect implies that light will be trapped (not totally) along particular caustic curves. Recently, transformation optics was proposed to manipulate light rays and waves freely [2,3]. There are many novel applications, such as cloaks [4,5], rotators [6], concentrators [7], and illusion devices [8–10]. The material parameters are anisotropic and inhomogeneous, thus the applications are only limited to microwaves and two dimensions [11–13]. Later, quasiconformal or conformal transformation optics became a better choice as the required material parameters are simply refractive-index profiles [2,14,15], and thus devices such as carpet cloaks and self-focusing lenses could be implemented at visible frequencies [16–18] and even in three dimensions [19,20]. The optics concept was extended to acoustic waves [21,22], surface water waves [23–25], and even thermal dynamics [26,27].

With regard to the previously mentioned caustic effect, as the light rays are confined along particular curves, it is possible to apply transformation optics to design new kinds of caustic devices with intriguing effects, which we call "transformation caustics." Under conformal mapping, such devices would require only refractive-index profiles and would thus be easier to implement.

In this article, we use two mappings as examples and transform a circular mirror and an elliptic mirror into a waveguide. The caustic curves are well transformed to desired curves, and even flat boundaries, which could be used to trap light and achieve either asymmetric propagation or cavities.

---

[*]kenyon@xmu.edu.cn

II. MAPPING FROM A CIRCULAR CAVITY

We start from an air cavity with a circular mirror. A light ray emitted from (x_0, y_0) in a particular direction will be reflected by the mirror, and will naturally form a circular caustic. Suppose the ray follows $y = kx + m$. When $k \to \infty$, the caustic is a circle with a radius of $|x_0|$. For other directions, the caustic has a radius of $\sqrt{m^2/(k^2 + 1)}$, as shown in Fig. 1(a). Under the conformal mapping $w = e^z$, the cavity will be transformed into a waveguide, with its refractive-index profile written as

$$n = e^x. \tag{1}$$

We plot the profile in Fig. 1(b). It ranges from e^{-2} to e^2. The starting point is mapped to the origin (0,0) and the trajectory of the transformed ray is mapped to a cycloidlike curve, as shown in Fig. 1(c). The circular caustic is now mapped to a flat boundary $x = (1/2) \ln[m^2/(k^2 + 1)]$ or $x = \ln |x_0|$, which means that the light will not reach the region lower than the boundary. The ray-tracing simulation is performed by COMSOL MULTIPHYSICS (for all other simulations below as well) and the asymmetric propagation is clearly demonstrated. In simulations, we take $x_0 = 1, y_0 = 0, k = 1, m = -1$, and a circular mirror with a radius of e^2, which is mapped to the upper boundary of the waveguide with $x = 2$. The lower boundary of the waveguide is set at $x = -2 < (1/2) \ln(1/2)$, which is related to a smaller circle inside the circular caustic. Since the radius of the circular caustic curve is very small, it would be reasonable to consider a point source instead of a light ray with a particular direction. In Fig. 1(d), we show the ray-tracing simulation for rays emitted from a point source. Although some of the rays could reach the lower part of the waveguide, the asymmetric propagation is still maintained. We also perform a full-wave simulation in the same structure; the electric field pattern is shown in Fig. 1(e). We consider a transverse electric mode with a wavelength of 1 m (could be an
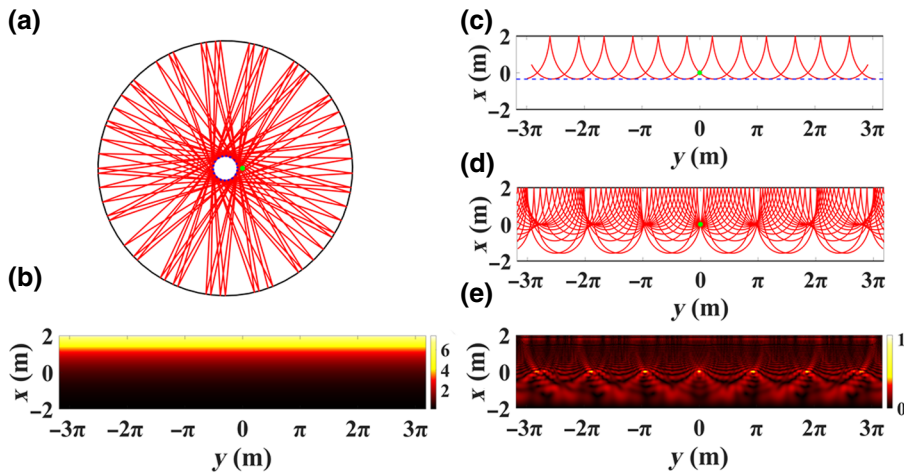
FIG. 1 (a) A ray from (1,0) in a direction of 45° will be reflected by the circular mirror (in black, with a radius of e^2) to form a caustic (the dashed blue circle with a radius of $1/\sqrt{2}$) inside. (b) The refractive-index profile of the transformed waveguide [Eq. (1)]. (c) A single transformed ray trajectory in the waveguide from the origin (0,0), with a flat caustic at $(1/2)\ln(1/2)$. (d) The transformed ray trajectories from a point source at the origin. (e) A full-wave simulation for a point source at the origin.

arbitrary unit) in the simulation. The point source is excited by a line-current source of 1 A and frequency of 1 GHz (the same values are used for all the following full-wave simulations). The pattern shows that more light waves will be confined to the upper part of the waveguide, consistent with the result of the ray-tracing simulation.

III. MAPPING FROM AN ELLIPTIC CAVITY

Now we provide another example, an air cavity with an elliptic mirror. All light rays from one of the focusing points will form an image at another focusing point [Fig. 2(a)]. Under a conformal mapping of $w = \cosh z$, it will be transformed into a waveguide with refractive-index profile

$$n = \sqrt{\sinh^2 x + \sin^2 y}, \tag{2}$$

where both outward boundaries are mapped from the elliptic mirror. We plot the profile in Fig. 2(b). In comparison with that in Fig. 1(b), it would be more feasible in practice. The two focusing points will be mapped to a series of points $(0, k\pi)$ along the x direction. Any point source at one of the focusing points will form images at other focusing points, as shown in Fig. 2(c). Here we set it at the origin (0,0). In this device the outward boundaries could be *arbitrary* at any x coordinate and are thus mapped to ellipses

with the same focusing points $(-1,0)$ and $(1,0)$, and the focusing effect will not change at all. We also perform a full-wave simulation in the same structure for a point source at the origin; the electric field pattern is shown in Fig. 2(d). At other transformed focusing points, the field amplitudes are strongly enhanced, which demonstrates the imaging functionalities clearly. The images are under the diffraction limit in this case, which is similar to the case for self-focusing lenses [18,28].

We suppose a light ray emitted from (x_0, y_0) follows $y = kx + m$. Under the following conditions, the ray will be reflected by the elliptic mirror and form an elliptic caustic, as shown in Fig. 3(a):

(a) When $k \neq 0$, $-(m/k)$ satisfies $1 < -(m/k) < \cosh x_1$ or $-\cosh x_1 < -(m/k) < -1$ (x_1 is an arbitrary constant related to the elliptic mirror).

(b) When $k = 0$, m satisfies $-\sinh x_1 < m < \sinh x_1$.

(c) When $k \to \infty$, $|x_0|$ satisfies $1 < |x_0| < \cosh x_1$ or $-\cosh x_1 < |x_0| < -1$.

After the above conformal mapping, asymmetric light propagation similar to that in the circular case shown in Fig. 1 will be achieved, as shown in Fig. 3(b). The caustic boundary is also flat. We take $x_0 = \cosh 1$, $y_0 = 0$, and $k \to \infty$ following condition (c) above in the simulation.
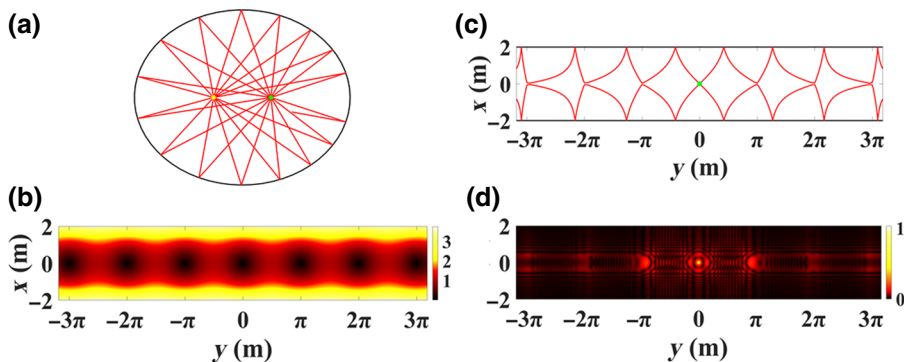

FIG. 2 (a) A point source at the focusing point of the elliptic mirror will form an image at another focusing point. (b) The refractive-index profile of the transformed waveguide [Eq. (2)]. (c) A point source at one of the transformed focusing points (e.g., the origin here) in the waveguide will form ray images at other transformed focusing points. (d) A full-wave simulation for a point source at the origin.
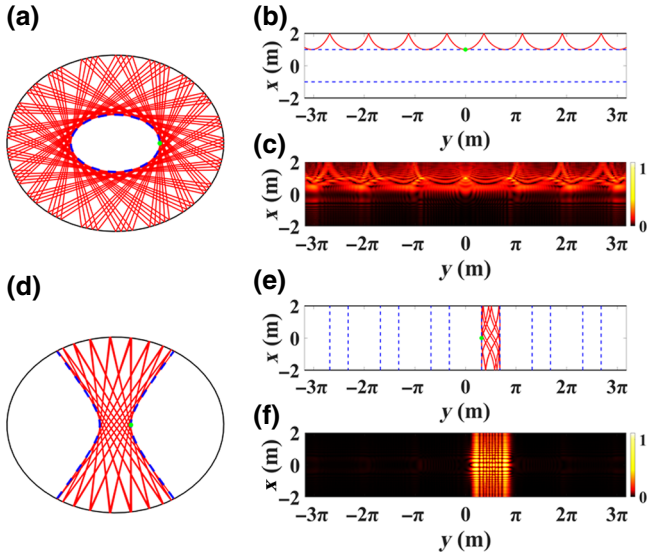
FIG. 3　(a) A ray emitted from (cosh 1, 0) in a direction of 90° will be reflected by the elliptic mirror to form an elliptic caustic. (b) The transformed ray trajectory from (a) in the refractive-index profile of Eq. (2) with a flat caustic at $x = 1$. (c) A full-wave simulation for the mapped point source at (1,0). (d) A ray emitted from (cos 1,0) in a direction of 90° will be reflected by the elliptic mirror to form two hyperbolic caustics. (e) The transformed ray trajectory from (d) in the refractive-index profile of Eq. (2) with two vertical caustics to confine the rays. (f) A full-wave simulation for the mapped point source at (0,1).

The elliptic mirror has a major axis of cosh 2 and a minor axis of sinh 2 (i.e., $x_1 = 2$), which is mapped to $x = 2$ and -2 (the upper and lower boundaries of the waveguide). If we put a point source at the mapped position (1,0), the asymmetric propagation of light will still be valid, with more rays penetrating into the lower part of the waveguide, as in Fig. 1(d). We show a full-wave simulation for the mapped point source in Fig. 3(c), where the asymmetric propagation is confirmed in wave optics.

However, for a light ray emitted from (x_0, y_0) with the following conditions, the ray will be reflected by the elliptic mirror and will be confined by two hyperbolic caustics, as shown in Fig. 3(d):

(a) When $k \neq 0$, $-(m/k)$ satisfies $-1 < -\frac{m}{k} < 1$.
(b) When $k \to \infty$, $|x_0|$ satisfies $-1 < x_0 < 1$.

After the mapping, it is amazing that the light will be trapped by two vertical boundaries, which is simply mapped from the two hyperbola, as shown in Fig. 3(e). We take $x_0 = \cos 1$, $y_0 = 0$, and $k \to \infty$ following condition (b) above in the simulation. In Fig. 3(f), we show a full-wave simulation for the mapped point source (0,1) to demonstrate the wave confinement. From the above discussions, we find that the caustic effect could be well used
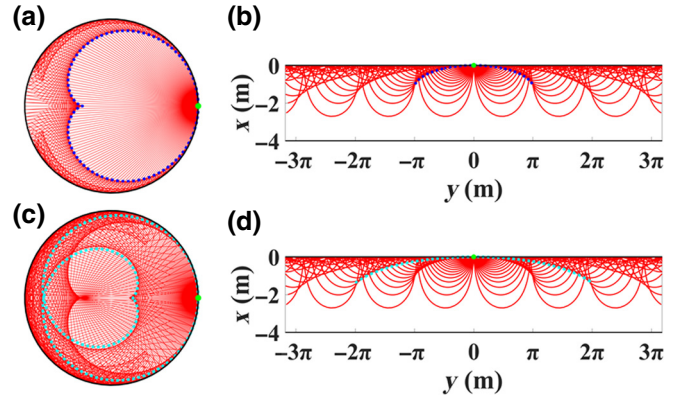

FIG. 4　(a) A point source at the outward boundary of the circular mirror (1,0) will be reflected by the mirror to form a cardioid caustic. (b) A point source in the refractive index profile of Eq. (1) will have a transformed caustic (dashed blue curve). (c) A second level of a cardioid caustic will be formed if the rays continue to propagate in (a). (d) The transformed caustic of the second level of a cardioid caustic.

to design devices for light trapping and confinement with the help of transformation optics.

IV. A MORE GENERAL CASE

Such a concept can go further. For the circular cavity, a point source at the outward boundary will be reflected by the mirror and form a cardioid caustic $[u = (2/3)\cos t(1 + \cos t) - (1/3), \ v = (2/3)\sin t(1 + \cos t)]$, as shown in Fig. 4(a). After the mapping of $w = e^z$, with the help of the refractive-index profile in Eq. (1), the caustic is transformed to a curve with $x = (1/2)\ln[4(1 + \cos t)^2 - 4\cos t(1 + \cos t) + 1] - \ln 3$ and $y = \arctan\{[2\sin t(1 + \cos t)]/[\cos t(1 + \cos t) - 1]\}$ in Fig. 4(b). We also find that there is a series of caustics along the x direction. This is caused by the second reflection or even multiple reflections by the mirror. For example, we plot the second reflection and find that it forms a two-level cardioid caustic $\{u = (3/4)\cos 4t[(1/3) + \cos t], v = (3/4)\sin 4t[(1/3) + \cos t]\}$ approximately, as shown in Fig. 4(c). Such a caustic is approximately transformed to a curve with $x = \ln[(1/4) + (3/4)\cos t]$ and $y = 4t$ with a larger width, as seen in Fig. 4(d). Similarly, one can obtain the transformed caustic for higher levels of reflection.

V. CONCLUSION

In summary, we show that by combining transformation optics, the caustic effect can be flexibly tuned to achieve asymmetric light propagation or even light trapping. Such an effect could lead to applications such as optical switches, energy concentrators, and microcativies. They could be implemented by gradient-index metamaterials [29,30]. With the help of recent nanotechnology

on metasurfaces [31], transformation caustics will become another method for light manipulation.

[1] V. I. Arnold, S. M. Guseĭn-Zade, and A. N. Varchenko, *Singularities of Differentiable Maps. Vol. I. The Classification of Critical Points, Caustics and Wave Fronts* (Monographs in Mathematics, 82. Birkhäuser Boston, Inc., Boston, MA, 1985).

[2] U. Leonhardt, Optical conformal mapping, Science **312,** 1777 (2006).

[3] J. B. Pendry, D. Schurig, and D. R. Smith, Controlling electromagnetic fields, Science **312,** 1780 (2006).

[4] S. A. Cummer, B.-I. Popa, D. Schurig, D. R. Smith, and J. Pendry, Full-wave simulations of electromagnetic cloaking structures, Phys. Rev. E **74,** 036621 (2006).

[5] D. Schurig, J. B. Pendry, and D. R. Smith, Calculation of material properties and ray tracing in transformation media, Opt. Express **14,** 9794 (2006).

[6] H. Y. Chen and C. T. Chan, Transformation media that rotate electromagnetic fields, Appl. Phys. Lett. **90,** 241105 (2007).

[7] M. Rahm, D. Schurig, D. A. Roberts, S. A. Cummer, D. R. Smith, and J. B. Pendry, Design of electromagnetic cloaks and concentrators using form-invariant coordinate transformations of Maxwell's equations, Photonics Nanostruct. – Fundam. Appl. **6,** 87 (2008).

[8] Y. Lai, J. Ng, H. Y. Chen, D. Han, J. Xiao, Z.-Q. Zhang, and C. T. Chan, Illusion Optics: The Optical Transformation of an Object Into Another Object, Phys. Rev. Lett. **102,** 253902 (2009).

[9] W. X. Jiang and T. J. Cui, Moving targets virtually via composite optical transformation, Opt. Express **18,** 5161 (2010).

[10] W. X. Jiang, H. F. Ma, Q. Cheng, and T. J. Cui, Virtual conversion from metal object to dielectric object using metamaterials, Opt. Express **18,** 11276 (2010).

[11] D. Schurig, J. J. Mock, B. J. Justice, S. A. Cummer, J. B. Pendry, A. F. Starr, and D. R. Smith, Metamaterial electromagnetic cloak at microwave frequencies, Science **314,** 977 (2006).

[12] H. Y. Chen, B. Hou, S. Chen, X. Ao, W. Wen, and C. T. Chan, Design and Experimental Realization of a Broadband Transformation Media Field Rotator at Microwave Frequencies, Phys. Rev. Lett. **102,** 183903 (2009).

[13] M. M. Sadeghi, S. Li, L. Xu, B. Hou, and H. Y. Chen, Transformation optics with Fabry-Pérot resonances, Sci. Rep. **5,** 8680 (2015).

[14] J. Li and J. B. Pendry, Hiding Under the Carpet: A New Strategy for Cloaking, Phys. Rev. Lett. **101,** 203901 (2008).

[15] L. Xu and H. Y. Chen, Conformal transformation optics, Nat. Photonics **9,** 15 (2015).

[16] J. Valentine, J. Li, T. Zentgraf, G. Bartal, and X. Zhang, An optical cloak made of dielectrics, Nat. Mater. **8,** 568 (2009).

[17] L. H. Gabrielli, J. Cardenas, C. B. Poitras, and M. Lipson, Silicon nanostructure cloak operating at optical frequencies, Nat. Photonics **3,** 461 (2009).

[18] X. Wang, H. Y. Chen, H. Liu, L. Xu, C. Sheng, and S. Zhu, Self-Focusing and the Talbot Effect in Conformal Transformation Optics, Phys. Rev. Lett. **119,** 033902 (2017).

[19] H. F. Ma and T. J. Cui, Three-dimensional broadband ground-plane cloak made of metamaterials, Nat. Commun. **1,** 21 (2010).

[20] T. Ergin, N. Stenger, P. Brenner, J. B. Pendry, and M. Wegener, Three-dimensional invisibility cloak at optical wavelengths, Science **328,** 337 (2010).

[21] S. A. Cummer and D. Schurig, One path to acoustic cloaking, New J. Phys. **9,** 45 (2007).

[22] H. Chen and C. Chan, Acoustic cloaking in three dimensions using acoustic metamaterials, Appl. Phys. Lett. **91,** 183518 (2007).

[23] M. Farhat, S. Enoch, S. Guenneau, and A. B. Movchan, Broadband Cylindrical Acoustic Cloak for Linear Surface Waves in a Fluid, Phys. Rev. Lett. **101,** 134501 (2008).

[24] H. Y. Chen, J. Yang, J. Zi, and C. T. Chan, Transformation media for linear liquid surface waves, Europhys. Lett. **85,** 24004 (2009).

[25] C. Li, L. Xu, L. Zhu, S. Zou, Q. Huo Liu, Z. Wang, and H. Chen, Concentrators for Water Waves, Phys. Rev. Lett. **121,** 104501 (2018).

[26] C. Z. Fan, Y. Gao, and J. P. Huang, Shaped graded materials with an apparent negative thermal conductivity, Appl. Phys. Lett. **92,** 251907 (2008).

[27] S. Guenneau, C. Amra, and D. Veynante, Transformation thermodynamics: Cloaking and concentrating heat flux, Opt. Express **20,** 8207 (2012).

[28] S. Tao, Y. Zhou, and H. Y. Chen, Maxwell's fish-eye lenses under Schwartz-Christoffel mappings, Phys. Rev. A **99,** 013837 (2019).

[29] Q. Wu, X. Feng, R. Chen, C. Gu, S. Li, H. Li, Y. Xu, Y. Lai, B. Hou, H. Y. Chen, and Y. Li, An inside-out Eaton lens made of H-fractal metamaterials, Appl. Phys. Lett. **101,** 031903 (2012).

[30] Y. Xu, Y. Fu, and H. Y. Chen, Planar gradient metamaterials, Nat. Rev. Mater. **1,** 16067 (2016).

[31] F. Zhong, J. Li, H. Liu, and S. Zhu, Controlling Surface Plasmons Through Covariant Transformation of the Spin-Dependent Geometric Phase Between Curved Metamaterials, Phys. Rev. Lett. **120,** 243901 (2018).